Journal of Vacuum Science and Technology B

RESEARCH ARTICLE | DECEMBER 21 2023

Analytic study of exposure contrast over feature edge in electron-beam lithography FREE

Special Collection: Papers from the 66th International Conference on Electron, Ion and Photon Beam Technology and Nanofabrication (EIPBN 2023)

Soo-Young Lee

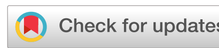

J. Vac. Sci. Technol. B 41, 062606 (2023)
https://doi.org/10.1116/6.0003029

View Online

Export Citation

CrossMark

27 December 2023 17:23:26

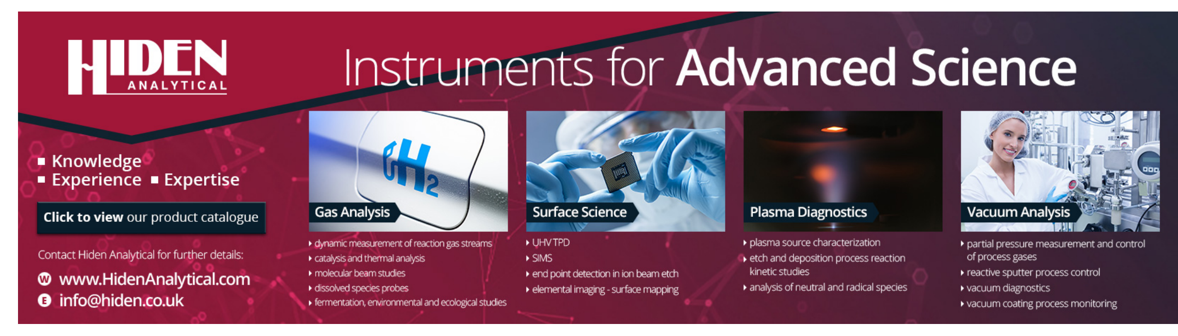

JVST B
Journal of Vacuum Science & Technology B
ARTICLE
pubs.aip.org/avs/jvb

Analytic study of exposure contrast over feature edge in electron-beam lithography

Cite as: J. Vac. Sci. Technol. B **41**, 062606 (2023); doi: 10.1116/6.0003029
Submitted: 31 July 2023 · Accepted: 21 November 2023 ·
Published Online: 21 December 2023

View Online Export Citation CrossMark

Soo-Young Lee[a)]

AFFILIATIONS

Department of Electrical and Computer Engineering, Auburn University, Auburn, Alabama 36849

Note: This paper is part of the Special Topic Collection: Papers from the 66th International Conference on Electron, Ion and Photon Beam Technology and Nanofabrication (EIPBN 2023).

[a)]**Electronic mail:** leesooy@auburn.edu

ABSTRACT

In electron-beam (e-beam) lithography, the location of a feature edge may vary with experiment due to the stochastic nature of the e-beam exposure and resist-development processes. From the viewpoint of consistent reproducibility of a circuit pattern, it is essential to enhance the stability of a feature edge in the e-beam lithographic process. A fundamental metric affecting the stability is the exposure contrast over the feature edge, and therefore, it is important to understand the dependency of exposure contrast on significant parameters. However, the computer simulation for the dependency analysis is time-consuming and needs to be repeated. In this study, a new method has been developed by deriving closed-form mathematical expressions of exposure contrast for the cases of a single feature and a uniform pattern of multiple features. The mathematical expressions enable the fast analysis of exposure contrast without simulation, and therefore, can serve as a useful tool in e-beam lithography.

Published under an exclusive license by the AVS. https://doi.org/10.1116/6.0003029

27 December 2023 17:23:26

I. INTRODUCTION

Electron-beam (e-beam) lithography has been one of the popular choices for transferring a pattern of fine features onto a substrate.[1–6] As the feature size continues to decrease, the accuracy of feature dimensions, such as critical dimension (CD), after the pattern transfer becomes even more important. The feature dimensions are measured according to the feature boundaries or edge locations. A source of CD error is the proximity effect due to the electron scattering in the resist, and a great deal of research effort has been put on the proximity effect correction (PEC). There are a number of effective PEC methods developed for e-beam lithography.[7–11] However, even with the optimal PEC result, the location of a feature edge may vary from experiment to experiment. This variation of edge location may be caused by the randomness in both e-beam exposure and resist-development processes; i.e., they are stochastic processes. An important metric directly related to the stability of edge location is the exposure contrast (EC) over the feature edge where the *exposure* refers to the e-beam energy deposited at a point in the resist.

In computational lithography, the spatial distribution of exposure (just *exposure distribution* hereafter) is computed point-by-point through the convolution between the dose distribution for a feature or a pattern and the point spread function (PSF) where the *dose* refers to the e-beam energy incident on a point on the top surface of resist and the PSF describes the exposure distribution within the resist when a point on the resist surface is exposed.[12] While this approach is flexible, one needs to carry out the time-consuming simulation (convolution) whenever any parameter is changed. Also, one cannot see an explicit relationship between the EC and a parameter until the simulation is repeated many times with the parameter varied.

The main objective of this study is to develop a new way to analyze the EC by deriving the mathematical expressions of EC, which allow one to avoid the shortcomings of the simulation-based approach. Such an analytic approach was not taken in any previous work, and a closed-form expression of EC is not currently available. For the simplicity of derivation, a double-Gaussian approximation of PSF is employed, and a long rectangular feature and a uniform pattern of such features, e.g., line/space (L/S) patterns, are assumed. However, as will be discussed later in Sec. VII, the double-Gaussian model of PSF is not a requirement for the results of this study to be valid. This paper describes in detail the derivation of a closed-form expression of EC as a function of lithographic and pattern

Published under an exclusive license by the AVS

parameters for a single feature and then that for a pattern based on the single-feature result. The parameters considered include the forward-scattering and backscattering ranges, the ratio of the back-scattered energy to the forward-scattered energy, edge location, feature-width reduction (for PEC), the number of line features in a pattern, etc. Also, examples of analyzing the dependency of EC on a parameter using the expressions for various cases are provided.

The significance of the results from this work includes: (1) They enable the fast analysis of EC without simulation, (2) they may be used with both analytic and numeric forms of PSF, and (3) they can be utilized in developing a PEC scheme with an emphasis on the edge stability of written features.

The rest of the paper is organized as follows. The model for the analytic study is depicted in Sec. II. The exposure and EC are introduced in Sec. III. The closed-form expression of EC for a single feature is derived in Sec. IV. The derivation of an EC expression for a pattern of multiple features is described in Sec. V. Several examples of analyzing the EC using the expressions are provided in Sec. VI. The results and their validity and significance are summarized in Sec. VII.

II. MODEL

When an e-beam is incident on a point on the resist surface, electrons from the beam travel through the resist being scattered and depositing their energy in the resist. The exposure distribution from exposing a single point is quantitatively described by the PSF. In this paper, for the simplicity of expression, the PSF is modeled with two 2D Gaussian functions as follows:

$$psf(x, y) = \frac{1}{\pi(1+\eta)}\left(\frac{1}{\alpha^2}e^{\frac{-(x^2+y^2)}{\alpha^2}} + \frac{\eta}{\beta^2}e^{\frac{-(x^2+y^2)}{\beta^2}}\right), \tag{1}$$

where α, β, and η are the forward-scattering and backscattering ranges and the ratio of the backscattered energy to the forward-scattered energy, respectively.

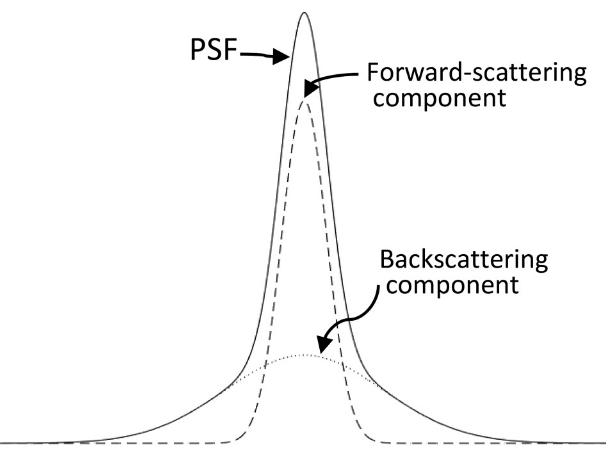

FIG. 1. Schematic diagram of PSF: the shapes of the forward-scattering and backscattering components are represented by the parameters α and β, respectively, as can be seen in Eq. (1).

In Fig. 1, a schematic diagram of PSF is provided. The overall shape of PSF is determined by the three parameters, α, β, and η, which depend on various factors, such as the beam energy, the beam diameter, the resist thickness, the substrate composition, etc. The exposure distribution due to the forward scattering of electrons is characterized by α and that due to the backscattering by β. The ratio of the exposure level of backscattering to that of forward scattering is denoted by η.

The variation of PSF along the resist depth dimension (Z) is not considered. Note that the variation is small in the case of thin resist. When the PSF does vary with Z, i.e., the resist layer, the EC can be derived for each layer, following the derivation procedure described in this paper.

In general, the exposure distribution $e(x, y)$ can be computed as

$$e(x, y) = \int\int psf(x - x', y - y')D(x', y')dx'dy', \tag{2}$$

where $D(x, y)$ describes the dose distribution for a feature or a pattern.

Consider a rectangular feature with width W and length L as illustrated in Fig. 2. Assume that the feature is sufficiently long in the Y dimension, e.g., $L \gg \alpha$. In such a case, the exposure depends only on x except in the regions close to the four corners of the feature. Then, the exposure distribution can be expressed as $e(x)$ along the X axis passing through the center of feature (see Fig. 2). Specifically, assuming that the dose does not vary with y, i.e., the uniform dose within the feature, $e(x)$ can be computed as

$$e(x) = \int h(x - x')D(x')dx', \tag{3}$$

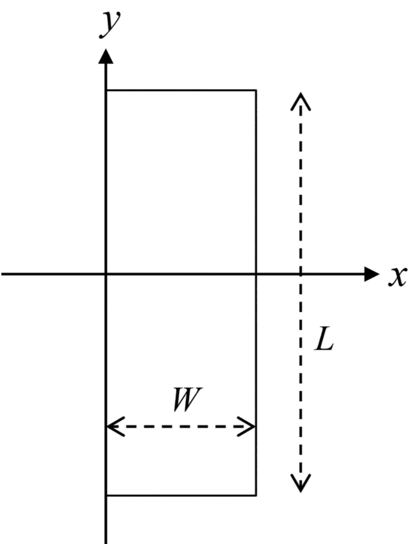

FIG. 2. Rectangular feature with width W and length L, which is long along the Y dimension.

27 December 2023 17:23:26

Published under an exclusive license by the AVS

where $h(x)$ is the *line spread function* (LSF) and $D(x)$ is the dose distribution over the feature width.

The line spread function is defined as

$$h(x) = \int_{-\infty}^{\infty} psf(x, y)dy = \frac{1}{\sqrt{\pi}(1+\eta)}\left(\frac{1}{\alpha}e^{\frac{-x^2}{\alpha^2}} + \frac{\eta}{\beta}e^{\frac{-x^2}{\beta^2}}\right). \quad (4)$$

That is, the LSF, $h(x)$, describes the exposure distribution when a long line of points is exposed with a uniform dose. In this study where long rectangular features, i.e., lines, are considered, the LSF is employed instead of the PSF. Note that the LSF is equivalent to the 1D PSF.

A pattern to be considered in this study consists of multiple long features or lines where the width of each line is W and the space between two adjacent lines is S as shown in Fig. 3. The period P is defined as $W + S$, which is fixed for a given pattern. The number of lines in a pattern is denoted by N where N is assumed to be odd. For simplicity, it is assumed that every feature is exposed with a uniform dose D_0, i.e., $D(x) = D_0$ within the exposed area and $D(x) = 0$ outside the exposed area. However, the results of this study are still applicable even in the cases where the dose varies within a feature (refer to Sec. VII) or among features in a pattern (refer to Sec. V).

It is worthwhile to point out that though a single Gaussian beam is implied as indicated in Eq. (1), the results from this study are still applicable to a shaped-beam of a rectangular aperture. Note that the exposure distribution from a rectangle-shaped beam is equivalent to that of a rectangular feature exposed by a single Gaussian beam.

III. EXPOSURE CONTRAST

The exposure contrast $EC(x)$ is defined as the rate at which the exposure changes at x in the direction of X and may be quantified by the slope of the exposure curve $e(x)$, i.e., the derivative of $e(x)$ with respect to x,

$$EC(x) = \frac{de(x)}{dx}. \quad (5)$$

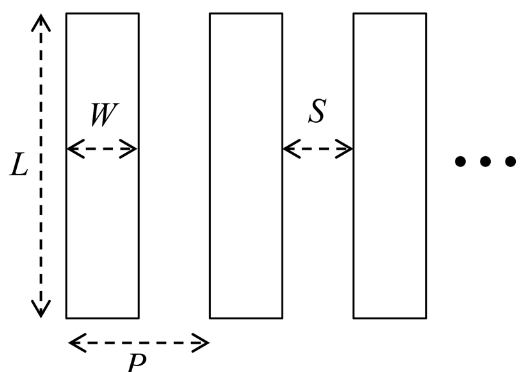

FIG. 3. L/S pattern where the width and length of each line are W and L, respectively, and the space between two adjacent lines is S.

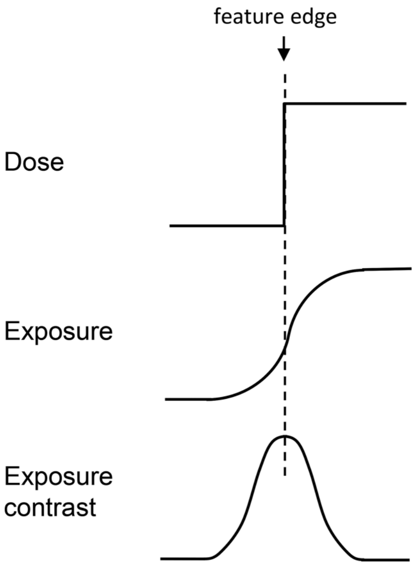

FIG. 4. Dose, exposure, and exposure contrast over the left edge of a feature.

In Fig. 4, the dose, exposure, and EC around the left edge of a feature are illustrated. It is shown in the figure that the maximum EC occurs at the middle point in the slope of exposure. This is usually the case assuming that the feature width is sufficiently large compared to the scattering ranges of electrons. However, as will be seen later, a deviation from this can happen in some cases depending on the values of certain parameters.

To understand the relationship between the EC and the stability of a feature-edge location, consider a simple resist-development model where a point (in the resist) above an exposure threshold is developed or remains undeveloped otherwise. The location of a feature edge can be affected by the (unintended) variation of dose, developing time, developer concentration, etc. All these variations may be equivalently converted into a variation of the exposure threshold. As illustrated in Fig. 5, for a higher EC, i.e., a steeper slope of exposure, the location of a feature edge would be moved less as the threshold goes up or down. That is, the higher the EC is, the smaller the variation of a feature-edge location becomes. Hence, in order to minimize the variation of the edge location, the EC is to be maximized along the target boundary (edge) of the feature.

IV. SINGLE FEATURE

Consider a long (line) feature with width W where its left and right edges are at $x = 0$ and $x = W$, respectively. A simple PEC technique is to reduce the feature width and expose the reduced feature area with a uniform dose D_0, which would result in the dose distribution illustrated in Fig. 6. Note that the width to be exposed is reduced by $2\Delta W$ (ΔW on each side of the feature), while the target width is still W.

27 December 2023 17:23:26

Published under an exclusive license by the AVS

FIG. 5. Variation (ΔX) of the edge location due to a change in the developing threshold of exposure is smaller for a higher exposure contrast.

The exposure distribution over the feature (refer to Fig. 6) can be computed as

$$e(x) = \int_0^W h(x - x')D(x')dx' = D_0 \int_{\Delta W}^{W-\Delta W} h(x - x')dx'. \quad (6)$$

Then, following the definition of EC,

$$EC(x) = \frac{de(x)}{dx} = D_0 \int_{\Delta W}^{W-\Delta W} \frac{dh(x - x')}{dx} dx'. \quad (7)$$

It is not difficult to show that the antiderivative of $\frac{dh(x-x')}{dx}$ with respect to x' is $-h(x - x')$. Therefore, by completing the integration in Eq. (7), the following result is obtained:

$$EC(x) = D_0[h(x - \Delta W) - h(x - W + \Delta W)]. \quad (8)$$

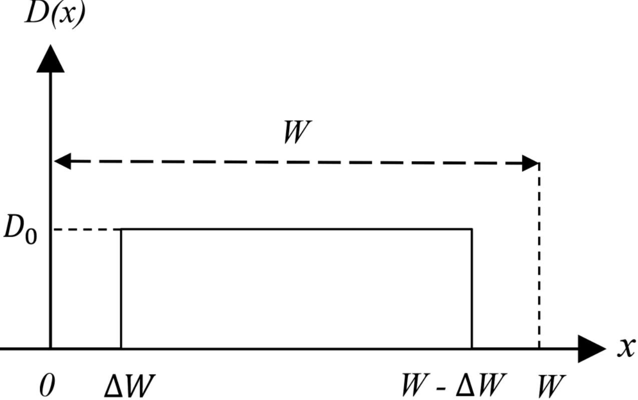

FIG. 6. Width of a feature is reduced by $2\Delta W$ for the PEC, and the reduced feature is exposed with a uniform dose of D_0.

Now, substituting the expression in Eq. (4) for $h(x)$ in Eq. (8) results in

$$EC(x) = \frac{D_0}{\sqrt{\pi}(1+\eta)} \left[\frac{1}{\alpha} \left(e^{\frac{-(x-\Delta W)^2}{\alpha^2}} - e^{\frac{-(x-W+\Delta W)^2}{\alpha^2}} \right) + \frac{\eta}{\beta} \left(e^{\frac{-(x-\Delta W)^2}{\beta^2}} - e^{\frac{-(x-W+\Delta W)^2}{\beta^2}} \right) \right]. \quad (9)$$

The result in Eq. (9) explicitly shows the dependency of the EC on the lithographic (α, β, and η) and pattern (W and ΔW) parameters.

It is worthwhile to appreciate the result in Eq. (8). Consider the case of $\Delta W = 0$. It is seen that the EC at the left target edge, $EC(0)$, is proportional to $h(0) - h(-W) = h(0) - h(W)$ [note that $h(x)$ is symmetric with respect to $x = 0$], i.e., determined by the difference between the two values of LSF at $x = 0$ and $x = W$, which correspond to the left and right ends of the exposed region (when the LSF is centered at $x = 0$, i.e., the peak of LSF, $h(0)$, is at $x = 0$), respectively. One can easily see that this interpretation still holds even when $\Delta W \neq 0$; i.e., $EC(0) = h(-\Delta W) - h(-W + \Delta W) = h(\Delta W) - h(W - \Delta W)$. Therefore, in general, $EC(0)$ is smaller for a larger ΔW as the difference of $h(\Delta W) - h(W - \Delta W)$ decreases as ΔW increases [note that $h(x)$ is monotonically decreasing from $h(0)$ in both directions].

The EC at the right target edge, $EC(W)$, is $h(W - \Delta W) - h(\Delta W)$, i.e., the same absolute value but with the opposite sign as that at the left target edge as expected. Note that the EC is positive at the left edge while negative at the right edge.

V. PATTERNS OF MULTIPLE FEATURES

The multiple-feature pattern considered in this study is an L/S pattern where each line is long in the Y dimension (refer to Fig. 3). As in the case of a single feature, the width of each feature (line) to be exposed may be reduced for the PEC and a uniform dose D_0 is given to all features in a pattern as illustrated in Fig. 7. Note that the left edge of the center line is at $x = 0$.

The exposure at a point can be computed as the sum of exposure contributions from all features in the pattern. Therefore,

$$e(x) = \int h(x - x')D(x')dx' = D_0 \sum_{i=-\lfloor N/2 \rfloor}^{\lfloor N/2 \rfloor} \int_{iP+\Delta W}^{iP+W-\Delta W} h(x - x')dx'.$$

Following the same derivation steps as for the single feature, one can get the following result:

$$\begin{aligned} EC(x) &= \frac{de(x)}{dx} \\ &= D_0 \sum_{i=-\lfloor N/2 \rfloor}^{\lfloor N/2 \rfloor} \int_{iP+\Delta W}^{iP+W-\Delta W} \frac{d\, h(x - x')}{dx} dx' \\ &= D_0 \sum_{i=-\lfloor N/2 \rfloor}^{\lfloor N/2 \rfloor} [h(x - iP - \Delta W) - h(x - iP - W + \Delta W)] \end{aligned} \quad (10)$$

27 December 2023 17:23:26

Published under an exclusive license by the AVS

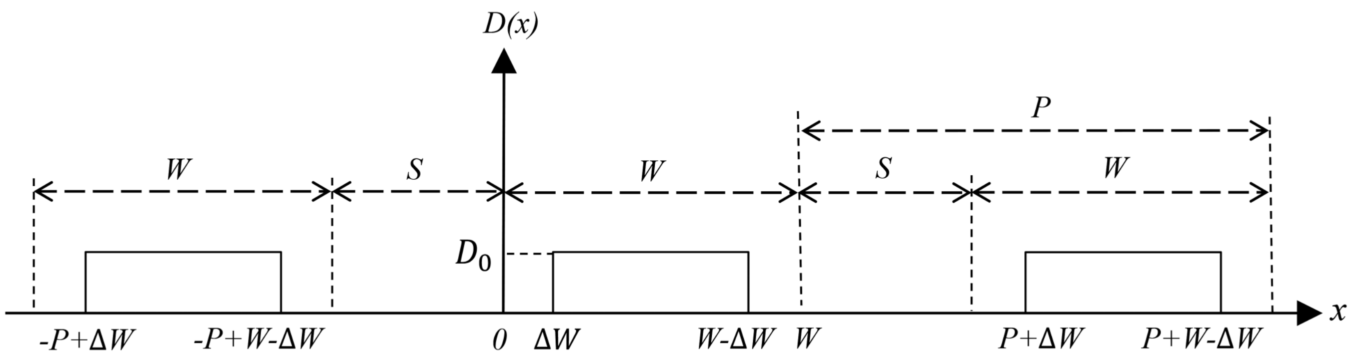

FIG. 7. Width of each line in an L/S pattern is reduced by $2\Delta W$ for the PEC, and all lines are exposed with a uniform dose of D_0. The period (P) of line/space pair is $W + S$.

$$= \frac{D_0}{\sqrt{\pi}(1+\eta)}\left[\sum_{i=-\lfloor N/2\rfloor}^{\lfloor N/2\rfloor}\left(\frac{1}{\alpha}\left(e^{\frac{-(x-iP-\Delta W)^2}{\alpha^2}} - e^{\frac{-(x-iP-W+\Delta W)^2}{\alpha^2}}\right)\right.\right.$$
$$\left.\left.+\frac{\eta}{\beta}\left(e^{\frac{-(x-iP-\Delta W)^2}{\beta^2}} - e^{\frac{-(x-iP-W+\Delta W)^2}{\beta^2}}\right)\right)\right]. \tag{11}$$

As can be seen in Eqs. (10) and (11), $EC(x)$ consists of the EC contributions from all features in the pattern. Some of the contributions are positive, while others are negative. For example, for the center feature, the contributions from the features on its left ($i < 0$) are negative, but those on its right ($i > 0$) are positive [note that $h(x)$ is smaller for a larger $|x|$]. Hence, as N increases, $EC(x)$ may not show monotonic behavior. Nevertheless, the EC at the left edge of the leftmost feature (which is positive) always increases as N increases. Similarly, the EC at the right edge of the rightmost feature (which is negative) always decreases as N increases. In any case, the exposure level increases as N increases. Therefore, it would be reasonable to normalize $EC(x)$ by $e(x)$ when analyzing the EC with N varied.

For the simplicity of equations, it is assumed in the above derivation that the feature-width reduction ΔW and dose are fixed for all features. When the ΔW or dose needs to be varied with each feature in a pattern as in a typical PEC result, the feature-dependent ΔW or dose can be easily incorporated into the derivation of EC, i.e., into Eqs. (10) and (11).

VI. ANALYSIS

The dependency of EC on the lithographic and pattern parameters is examined for several cases to demonstrate the usefulness of the closed-form expressions derived in this study. That is, in each case, the EC is computed directly from the expressions without any simulation.

In Fig. 8, the exposure, EC, and relative EC are plotted over the left edge of a single feature. The relative EC is defined as the EC divided by the exposure. As expected, the peak of EC occurs at the middle of the slope in the exposure curve, which corresponds to the target edge location. The EC defined in Eq. (5) is the absolute change rate of exposure, i.e., the absolute EC, and would be larger for a higher exposure level for the same percent change. Also, when the exposure level is lower, the EC can be smaller, though the percent change of exposure is larger. Therefore, one may be interested in the relative EC in addition to the (absolute) EC. As can be seen in Fig. 8, the peak of the relative EC does not occur where the EC is highest, but is maximized outside of the feature (exposed region). It would make sense to consider the relative EC when comparing two cases with different exposure levels.

In Fig. 9, the EC is plotted for the cases where the feature width ($W = 8$ nm) is comparable to the forward-scattering range ($\alpha = 3, 6$ nm). It is observed that the peak of EC is shifted to the left out of the exposed region, i.e., the peak is not at the target edge. Also, the EC is not symmetric with respect to the target edge. These are more conspicuous when $\alpha = 6$ nm than when $\alpha = 3$ nm.

27 December 2023 17:23:26

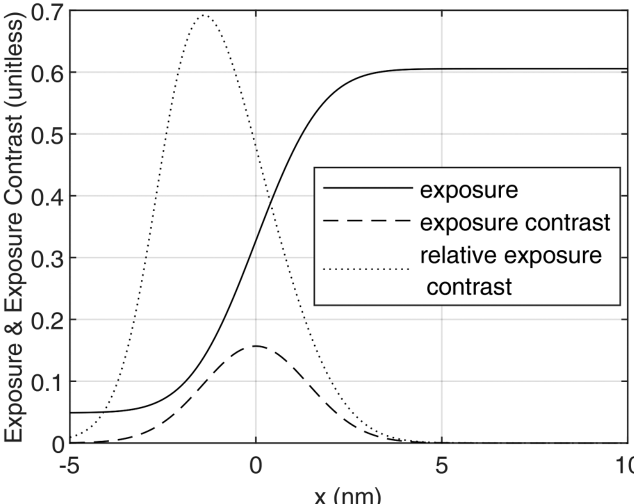

FIG. 8. Exposure distribution and contrast over the left edge (X= 0) of a single line: $\alpha = 2$ nm, $\beta = 100$ nm, $\eta = 0.8$, $W = 20$ nm, and $\Delta W = 0$.

Published under an exclusive license by the AVS

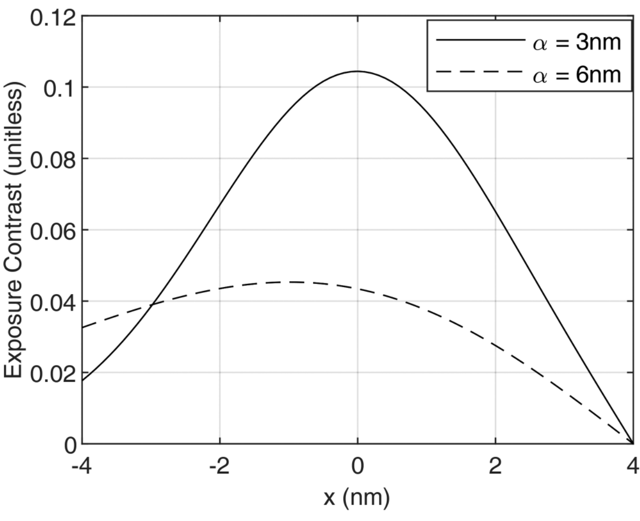

FIG. 9. Exposure contrast over the left edge ($X = 0$) of a single line: $\beta = 100$ nm, $\eta = 0.8$, $W = 8$ nm, and $\Delta W = 0$ (two different forward-scattering ranges, α, are considered).

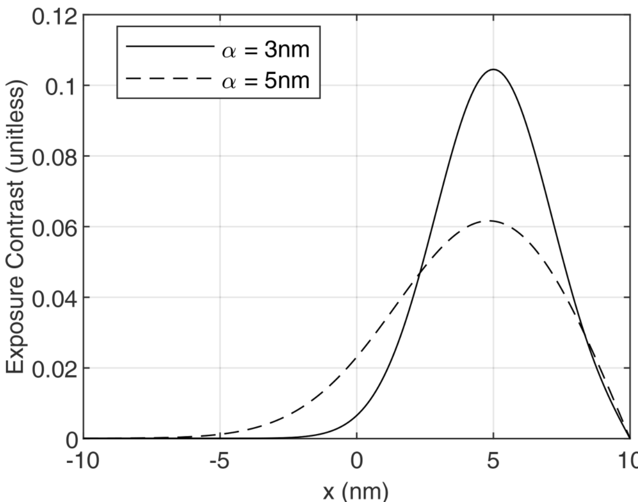

FIG. 11. Exposure contrast over the left edge ($X = 0$) of a single line: $\beta = 100$ nm, $\eta = 0.8$, $W = 20$ nm, and $\Delta W = 5$ nm (two different forward-scattering ranges, α, are considered).

In Fig. 10, the EC at the left edge of a single feature is analyzed as a function of feature-width reduction. As the width of the feature to be exposed is reduced, the EC decreases. This is a downside of the PEC method which shrinks a feature since the instability of edge location is increased. The decreasing rate of the EC is larger for a sharper LSF (i.e., a smaller α). For a broader LSF, the exposure level is maintained well into the unexposed region, which leads to a higher EC. Note that in the case of a sharper LSF, the exposure level quickly decreases at the feature edge, which is in the unexposed region, as ΔW increases.

In Fig. 11, the EC in the left edge region of a single feature is plotted for a given reduction of feature width ($\Delta W = 5$ nm). As expected, the peak of EC moves to the right by ΔW into the feature; i.e., the EC is not maximum at the feature edge.

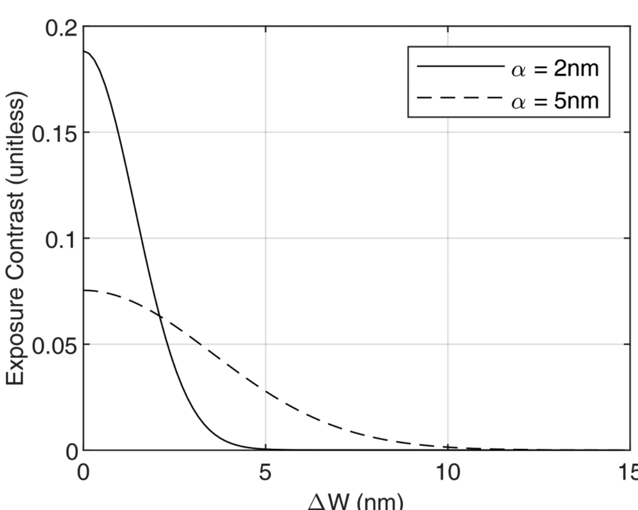

FIG. 10. Exposure contrast at the left edge of a single line as a function of line-width reduction (ΔW on each side) for the shape correction of PEC: $\beta = 100$ nm, $\eta = 0.5$, $W = 30$ nm, and $X = 0$ nm (two different forward-scattering ranges, α, are considered).

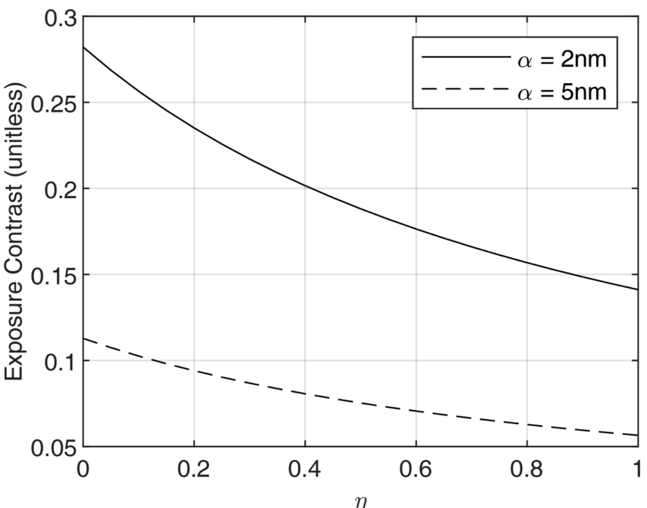

FIG. 12. Exposure contrast at the left edge of a single line: $\beta = 100$ nm, $W = 20$ nm, $\Delta W = 0$ nm, and $X = 0$ nm (two different forward-scattering ranges, α, are considered).

27 December 2023 17:23:26

Published under an exclusive license by the AVS

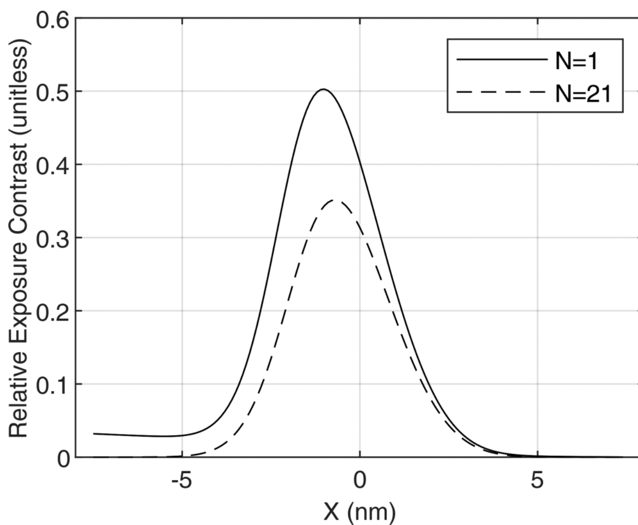

FIG. 13. Relative exposure contrast over the left edge of the center line in an L/S pattern: $\alpha = 2$ nm, $\beta = 30$ nm, $\eta = 0.8$, $W = 15$ nm, $S = 15$ nm, and $\Delta W = 0$ nm.

In Fig. 12, the dependency of EC on the back-scattered energy ratio (η) is examined at the left edge of a single feature. As η increases, the contribution of the back-scattered energy, which has a broader distribution compared to the forward-scattered energy, becomes greater. This makes the overall shape of LSF broader, leading to a slower-varying exposure distribution, resulting in a lower EC.

In Fig. 13, the relative EC over the left edge of the center line in an L/S pattern is plotted for two different pattern sizes ($N = 1, 21$). With the same dose given to all lines, the exposure level is higher in a larger pattern ($N = 21$) than in a single line ($N = 1$), and therefore, the relative EC is considered for a fair comparison. Overall, the relative EC is lower for the larger pattern. As discussed earlier, the EC contributions from other lines tend to cancel each other or even decrease the EC. In general, for a greater N, the spatial distribution of exposure gets smoothed out more (relative to the exposure level), leading to a lower relative EC. The peaks of the relative EC are outside of the exposed region, i.e., not at the feature edge, as in the case of a single line.

In Fig. 14, the relative EC at the left edge of the center line in an L/S pattern is observed as a function of N. It decreases quickly initially and then levels out as N increases. This behavior is related to the shape of LSF, which decreases fast from the peak and then becomes almost flat. The EC contribution from other line gets increasingly smaller as the distance to the line increases. Hence, as more lines are added, their effects on the relative EC diminish fast. The diminishing rate is larger for a sharper LSF as can be seen in the figure.

In Fig. 15, the effect of period ($P = W + S$) in an L/S pattern on the EC at the left edge of the center line is considered with W fixed. The larger the period is, the longer the distance between lines is. As P (equivalently S) increases, the negative effects from other lines on the EC decrease, and therefore, the EC increases. The increasing rate (and the increase itself) of EC is larger for a sharper LSF (a smaller α). For a broader LSF (a larger α), the effect of a line reaches farther. Hence, the EC still increases for a larger P, though the total increase is relatively smaller.

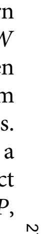

VII. SUMMARY

The EC is an important metric in e-beam lithography, which affects the stability of the feature-edge location. The dependency of

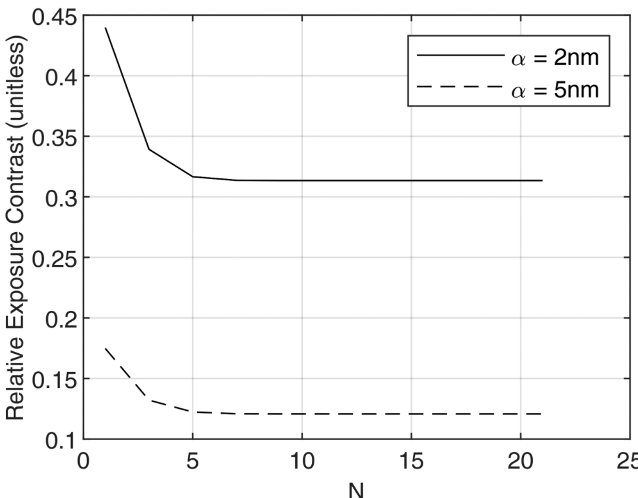

FIG. 14. Relative exposure contrast at the left edge of the center line in an L/S pattern: $\beta = 30$ nm, $\eta = 0.8$, $W = 10$ nm, $S = 10$ nm, $\Delta W = 0$ nm, and $X = 0$ nm (two different forward-scattering ranges, α, are considered).

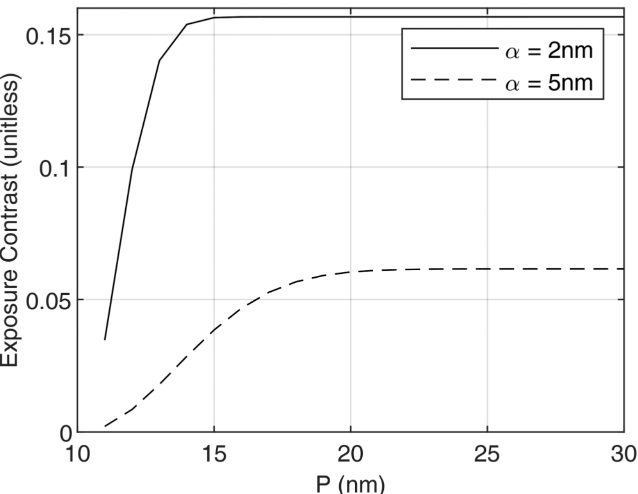

FIG. 15. Exposure contrast at the left edge of the center line in an L/S pattern: $\beta = 30$ nm, $\eta = 0.8$, $W = 10$ nm $\Delta W = 0$ nm, $N = 50$, and $X = 0$ nm (two different forward-scattering ranges, α, are considered).

Published under an exclusive license by the AVS

EC on the lithographic and pattern parameters may be examined through computer simulation. However, the time-consuming simulation has to be repeated for each individual case. In this study, the closed-form mathematical expressions of EC have been derived for the cases of a single feature and L/S patterns to provide a general method to analyze the EC without any simulation. Also, the usefulness of the expressions has been demonstrated by analyzing the behaviors of EC in terms of various parameters.

In this paper, it is assumed for the simplicity of derivation that each feature is exposed with a uniform dose. However, it is not difficult to see that the same derivation method can be employed for a nonuniform dose distribution. A feature may be partitioned into regions such that the dose is uniform within each region. A closed-form expression is derived for each region as in this study, and then the expressions for all the regions can be combined to get an expression for the whole feature.

It should be pointed out that the results of this study are still valid even when the LSF (equivalently PSF) is not modeled by a double-Gaussian approximation. First, if the LSF includes more than two Gaussian functions for higher accuracy, the additional Gaussian terms just need to be included in Eqs. (9) and (11). Second, the LSF may be modeled with any other types of functions than Gaussian functions, and the closed-form expressions can be obtained directly from Eqs. (8) and (10) as derived in this paper. Third, even when the LSF is given in a numeric format (as in the cases where the LSF or PSF is generated by Monte Carlo simulation or from the experimental data), the general expressions in Eqs. (8) and (10) can be utilized to compute the EC. Therefore, the analytic results presented in this paper are applicable to any form of LSF and allow one to avoid the point-by-point convolution (required in the simulation) in analyzing the EC.

An example of practical application is the development of a PEC scheme where high stability of a feature-edge location is required. The equations of EC can be used to determine the feature-width reduction or dose modulation, which achieves the maximum or high-enough EC at feature edges, without having to perform time-consuming simulation.

Considering the novelty of the approach, the generality of the results, and the applicability in the PEC, it may be said that this study has made a solid contribution to the field of e-beam lithography.

AUTHOR DECLARATIONS

Conflict of Interest

The author has no conflicts to disclose.

Author Contributions

Soo-Young Lee: Conceptualization (lead); Formal analysis (lead); Investigation (lead); Methodology (lead); Software (lead); Visualization (lead); Writing – original draft (lead); Writing – review & editing (lead).

DATA AVAILABILITY

The data that support the findings of this study are available within the article.

REFERENCES

[1] F. J. Hohn, J. Vac. Sci. Technol. B **7**, 1405 (1989).
[2] C. Vieu, F. Carcenac, A. Pepin, Y. Chen, M. Mejias, A. Lebib, L. Manin-Ferlazzo, L. Courraud, and H. Launois, Appl. Surf. Sci. **164**, 111 (2000).
[3] M. Aktary, M. O. Jensen, K. L. Westra, M. J. Brett, and M. R. Freeman, J. Vac. Sci. Technol. B **21**, L5 (2003).
[4] B. Bilenberg, S. Jacobsen, M. S. Schmidt, L. H. D. Skjolding, P. Shi, P. Boggild, J. O. Tegenfeldt, and A. Kristensen, Microelectron. Eng. **83**, 1609 (2006).
[5] C. M. Kolodziej and H. Maynard, Chem. Mater. **24**, 774 (2012).
[6] A. Chaker, H. R. Alty, P. Tian, A. Kotsovinos, G. A. Timco, C. A. Muryn, S. M. Lewis, and R. E. P. Winpenny, ACS Appl. Nano Mater. **4**, 406 (2021).
[7] R. Rau, J. H. McClellan, and T. J. Drabik, J. Vac. Sci. Technol. B **14**, 2445 (1996).
[8] B. D. Cook and S.-Y. Lee, IEEE Trans. Semicond. Manuf. **11**, 117 (1998).
[9] M. Osawa, K. Takahashi, M. Sato, H. Arimoto, K. Ogino, H. Hoshino, and Y. Machida, J. Vac. Sci. Technol. B **19**, 2483 (2001).
[10] T. Klimpel, M. Schulz, R. Zimmermann, H.-J. Stock, and A. Zepka, J. Vac. Sci. Technol. B **29**, 06F315 (2011).
[11] Q. Dai, S.-Y. Lee, S.-H. Lee, B.-G. Kim, and H.-K. Cho, J. Vac. Sci. Technol. B **30**, 06F307 (2012).
[12] S.-Y. Lee and B. D. Cook, IEEE Trans. Semicond. Manuf. **11**, 108 (1998).

27 December 2023 17:23:26

Published under an exclusive license by the AVS